

A 10 GHZ SPACE POWER COMBINER WITH PARASITIC INJECTION LOCKING

Robert J. Dinger, David J. White, and Donald Bowling

Michelson Laboratory, Physics Division
Naval Weapons Center, China Lake, CA 93555

ABSTRACT

An array of three microstrip patch antennas, each connected by a matching network to an IMPATT diode, has been investigated. Coherent radiation from the array was obtained at 10.23 GHz by feeding only the center element with an injection-locking signal, which then appeared at the input to the other two elements by free space mutual coupling. The three IMPATTs injection locked successfully in this manner. A beamwidth of 38 degrees and sidelobe level of -10 dB were achieved, values consistent with the theory for coherent radiation from an array of this configuration. An RF efficiency of 90% and a bandwidth of 30 MHz were measured.

INTRODUCTION

One of the problems in the development of solid-state transmitters is the design of efficient power combining structures. Individual solid-state diodes generate relatively low RF power levels (typically a few watts), and the outputs of many of these devices must be combined to achieve the tens or hundreds of watt levels required in radar systems.

Most combiner research has concentrated on closed structures, such as cavities or transmission lines; the diodes are coupled to this closed region, and the summed power is extracted at a single output port. If the power combiner output is ultimately radiated by an antenna array, then a closed combiner structure must be followed by a feed network for routing the signals to the array elements. Since the closed combining region and the feed network are efficiency-reducing sources of dissipative loss, for radiation applications it would be desirable to locate the diodes directly at the terminals of the array elements and combine the output power of the diodes "in free space," i.e. in the far field of the array. This type of array is referred to as a space power combiner.

This paper describes a space power combiner consisting of three microstrip patch antennas, each element of which has a single IMPATT diode connected to its terminal (Fig. 1). If allowed to free-run, each diode would oscillate with a frequency, power level, and RF phase that depend on the circuit impedance and specific diode conditions; the array would radiate incoherently. To force the IMPATTs to radiate coherently, an injection-locking signal must be supplied at the input to the diode. However, rather than piping an injection-locking signal

individually to each diode, the scheme in Fig. 1 requires only a single injection-locking signal applied to the center element. The injection-locking signal for the diodes at the terminals of the other elements appears by free-space mutual coupling between the elements. In principle, the technique is similar to the methods used to phase-lock arrays of semiconductor diode lasers (1). A complete discussion of the results presented below can be found in (2).

THEORY

The array shown in Fig. 1 is redrawn in a scattering matrix formalism in Fig. 2. Ports 1, 2, and 3 of [S] represent the three-element feeds of the array, and Port 4 represents the far-field measurement port where coherent power combining is desired. The circulator on arm 1 allows the injection-locking signal E to be introduced. The circulator and adjustable short in arms 2 and 3 form a reflection phase shifter for beam scanning. The diode and its impedance matching network are together represented by a reflection coefficient r_i that is greater than one.

The goal of the analysis is to determine the impedance that the array must present to the diodes to assure oscillation of the diodes in a desired mode. Hardware limitations in the realization of this impedance impact the bandwidth and other array characteristics. The scattering matrix [S] of the antenna array, assuming reciprocity and the appropriate symmetry, can be written

$$[S] = \begin{bmatrix} S_{11} & S_{12} & S_{13} & S_{14} \\ S_{12} & S_0 & S_{23} & S_{24} \\ S_{13} & S_{23} & S_0 & S_{34} \\ S_{14} & S_{24} & S_{34} & S_{44} \end{bmatrix} \quad (1)$$

where $S_{22} = S_{33} = S_0$. The lengths ℓ_2 and ℓ_3 in arms 2 and 3 are selected so that the phase factor in arm 2 (relative to the arm 1) is $\exp(-j\phi)$ and in arm 3 is $\exp(j\phi)$. Incorporating this constraint, assuming that $a_4 = 0$ (no external signal is incident on the array), and substituting $S_{24} = S_{14} \exp(-j\beta d \sin\theta)$ and $S_{34} = S_{14} \exp(j\beta d \sin\theta)$ (for a pattern angle θ in the H-plane, where d = element separation and $\beta = 2\pi/\lambda$) lead to the following equation for b_4 :

$$b_4 = S_{14}\Gamma_1 E \times$$

$$\left[1 + \frac{S_{12}\Gamma_2(\gamma_3 + S_{23}e^{j\phi}\Gamma_3)}{\gamma_2\gamma_3 - S_{23}\Gamma_2\Gamma_3} e^{-j(\beta d \sin\theta + \phi)} + \frac{S_{12}\Gamma_3(\gamma_2 + S_{23}e^{-j\phi}\Gamma_2)}{\gamma_2\gamma_3 - S_{23}\Gamma_2\Gamma_3} e^{j(\beta d \sin\theta + \phi)} \right] \quad (2)$$

where $\gamma_2 = 1 - S_0 e^{-j\phi\Gamma_2}$ and $\gamma_3 = 1 - S_0 e^{j\phi\Gamma_3}$. This equation is in the form of an antenna array factor: Each of the three terms is proportional to the element currents, multiplied by a phase factor accounting for the phase separation of the elements ($\beta d \sin\theta$) and the beam scan phase (ϕ) (although ϕ also appears in the element current factors). The quantity b_4 represents the combined power appearing in the far field and is directly proportional to the injection locking signal E . However, there can be a finite b_4 even when $E = 0$ if the denominators in terms two and three are zero, i.e. when

$$\gamma_2\gamma_3 - S_{23}\Gamma_2\Gamma_3 = 0 \quad (3)$$

This is a free-run oscillation condition. It is a condition that should be met for best performance even when an injection-locking signal is applied, since Eq. (2) implies that less injection signal is required for a given output as Eq. (3) is more closely satisfied.

In practice, of course, a zero denominator in Eq. (3) and the resulting "infinite" value of b_4 are not realized. The oscillation condition produces reflection coefficients greater than one, and hence power generation, but the power generated by each diode saturates at some limiting value. A theory that accounts for this behavior, and that thereby gives an estimate of power levels generated in the far field, requires a nonlinear model of the diode. The inclusion of diode models in the theory is currently in progress.

For given values of the entries in $[S]$, Eq. (3) indicates that an unlimited number of combinations of Γ_2 and Γ_3 can satisfy the oscillation condition. The principal objective here is a well-formed broadside beam; hence, symmetry requires that $\Gamma_2 = \Gamma_3$, as evaluated at broadside. Setting $\phi = 0$ in Eq. (3) and $\Gamma_2 = \Gamma_3 = \Gamma_0$ and solving for Γ_0 leads to

$$\Gamma_0^\pm = (S_0 \mp S_{23})^{-1} \quad (4)$$

To emphasize: Γ_0 is the desired reflection coefficient that the IMPATT diode, as transformed by its matching network, should present to the antenna array in order to satisfy the oscillation condition for $\phi = 0$.

EXPERIMENTAL ARRANGEMENT

Figure 3 is a photograph of the experimental array, and Table 1 summarizes some of its characteristics.

Table 1.

Center frequency, GHz	10.2
Element spacing, λ	0.47
Input impedance, λ	45 + j14
Adjacent element coupling, dB	-13
Bandwidth, MHz	300

Transformation of the approximate $-0.5 + j4$ ohm impedance of a typical IMPATT diode to the line impedance of 50 ohms was accomplished using a single section of low-impedance transmission line. The diode mounts, with integral transformer and cooling jacket, are visible in the rear of Fig. 3.

For Fig. 4, the entries in $[S]$ measured for the experimental array were substituted into Eq. (4), converted to impedance, and plotted as a function of frequency. Also shown are curves for a typical diode impedance as transformed by the low-impedance transformer. These curves indicate that a reasonably acceptable match is achieved between antenna array and diode over a frequency span of 10.25 to 10.35 GHz.

The IMPATT diodes were operated in a pulsed mode (50% duty cycle at 500 kHz). Measurements of the far-field spectra and antenna patterns were made in an anechoic chamber.

EXPERIMENTAL RESULTS

Figure 5 shows the spectrum of the far-field signal when no injection-locking signal was present; each diode free runs, and the array is incoherent. Next, an injection-locking signal was supplied to the center element at a frequency of 10.230 GHz and a power level of 0.55 W. All diodes were driven at the same current level, and an H-plane pattern measurement was made. Figure 6 shows the result. A beam with a 3-dB width of 36 degrees was formed at broadside. The beamwidth and sidelobe level agree well with simple array theory, which predicts a beamwidth of 38 degrees and -10 sidelobe level. In Fig. 7, we show the spectrum of the signal measured in the far field during the pattern measurement for Fig. 6. A single peak results because of the injection locking, confirming array coherency.

We define the array efficiency as $\epsilon = 100\% \times (\text{total radiated power}) / (\text{RF power generated by the IMPATT diodes})$. The RF power generated by each IMPATT diode was measured as 3.2 W, 3.0 W, and 3.7 W, yielding a total RF power generated by diodes of 9.9 W. The total radiated power, obtained in the standard manner by integrating the measured pattern, was 8.98 W. Hence, the computed efficiency is $\epsilon = 90.9\%$.

The bandwidth was measured by varying the injection-locking frequency and observing the breakup of the main beam and loss of coherency in the far field spectrum. Array coherency was found to be maintained between 10.22 and 10.25 GHz, establishing the array locking bandwidth as 30 MHz.

We conducted some preliminary experiments to investigate scanning of the beam. A constant interelement phase shift was provided by precision

fixed shorts that were connected as shown in Fig. 2 to the circulators on elements 2 and 3. A disadvantage of this method is the transformation in antenna terminal impedance viewed by the IMPATT diode because of the extra line length of the shorts. Beyond some electrical length, the impedance will be transformed out of the coherent locking range of the diodes. Or, from the point of view of Eq. (4), the oscillation condition is not satisfied.

A scanned beam pattern is shown in Fig. 8 for an interelement phase shift of 60 degrees. The beam scans in the desired manner to 29 degrees; the amount of shift agrees well with the 25-degree scan angle predicted by elementary phased array theory. However, an interelement phase shift of 60 degrees is near the scan limit for this array. For greater phase shifts, the impedance transformation produced by the electrical length of the shorts causes the IMPATT diodes to unlock. Measurements of the spectrum of the far field confirmed this.

CONCLUSIONS

Coherent radiation and a well-formed beam were obtained from the array of three-microstrip patch antennas. Work is currently in progress to extend the parasitic injection-locking technique to larger arrays.

At least three advantages accrue from this exploitation of the free-space coupling. First, the weight, bulk, and complication of transmission lines for an injection-locking signal for each element are eliminated. Second, a circulator is not required on each element for feeding of the injection-locking signal. And third, the technique is better suited for planar integrated antennas because these extra components are not required.

REFERENCES

- (1) D. Botez and D. Ackley, "Phase-Locked Arrays of Semiconductor Diode Lasers," *IEEE Circuits and Devices Magazine*, January 1986.
- (2) R. Dinger, D. White, and D. Bowling, "A 10-GHz Space Power Combiner with Parasitic Injection Locking," Naval Weapons Center Technical Publication 6704, March 1986.

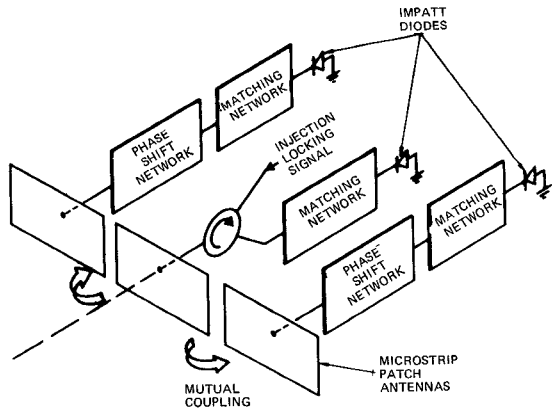


Fig. 1. Transmitting Array with Parasitic Injection Locking.

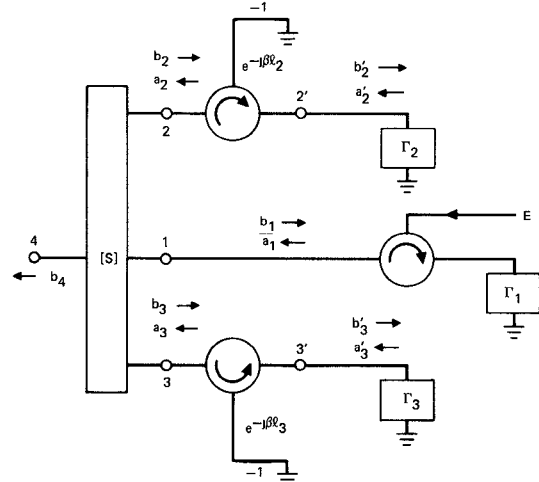


Fig. 2. Array Circuit.

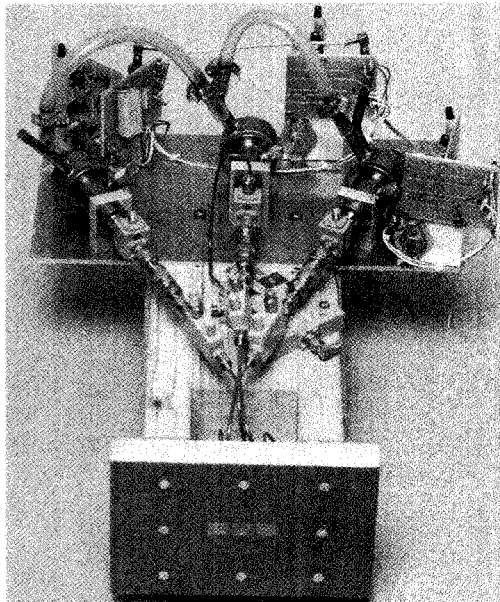


Fig. 3. Experimental Array.

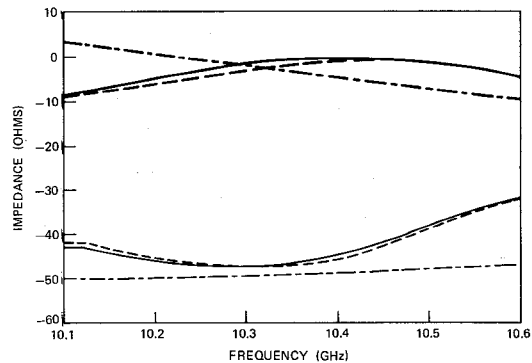


Fig. 4. Impedance vs. Frequency. Heavy curves are reactance; lighter curves are resistance. Solid curves, + root of Eq. (4); dashed curves, - root of Eq. (4); dash-dot curves, transformed diode impedance.

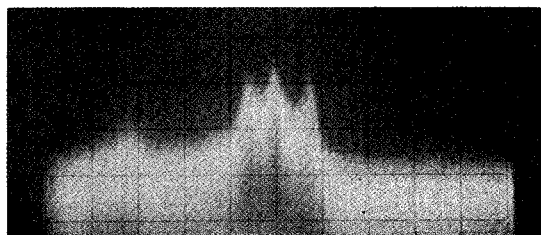


Fig. 5. Far-Field Spectrum with Injection-Locking Signal Removed. Horizontal scale = 10 MHz/div.

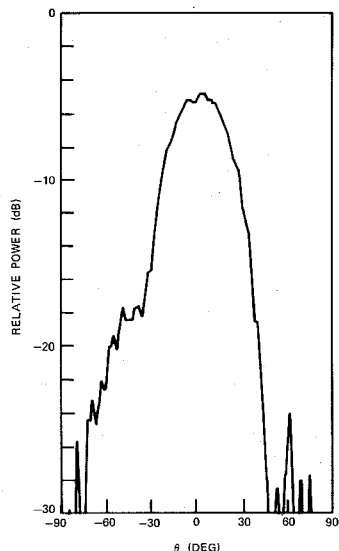


Fig. 6. Measured Array Pattern.

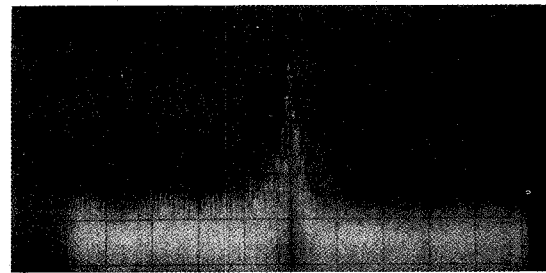


Fig. 7. Far-Field Spectrum with Injection-Locking Signal Applied. Horizontal scale = 10 MHz/div.

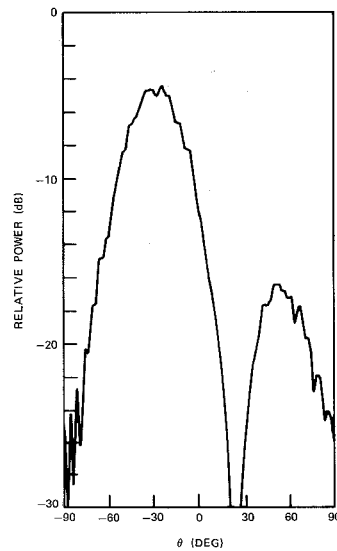


Fig. 8. Measured Array Pattern for Interelement Phase Shift of 60 degrees.